International Conference on Mathematics, Computational Methods & Reactor Physics (M&C 2009)
Saratoga Springs, New York, May 3-7, 2009, on CD-ROM, American Nuclear Society, LaGrange Park, IL (2009)

APPLICATION OF ELECTRON DOSE KERNELS TO ACCOUNT FOR HETEROGENEITIES IN VOXELIZED PHANTOMS

Ahmad K. Al-Basheer[1,2], Glenn E. Sjoden[1], Monica Ghita[3], and Wesley Bolch[1]
akas30@ufl.edu, sjoden@ufl.edu, ghita1mc@ufl.edu, wbolch@ufl.edu
[1]University of Florida, Dept of Nuclear & Radiological Engineering, Gainesville, Florida 32611
[2]Georgia Radiation Therapy Center, Medical College of Georgia, Augusta, Georgia 30912
[3]University of Florida, Dept of Radiology, Gainesville, Florida 32611

ABSTRACT

In this paper, we present work on the application of the Electron Dose Kernel discrete ordinates method (EDK-S_N) to compute doses and account for material heterogeneities using high energy external photon beam irradiations in voxelized human phantoms. EDKs are pre-computed using photon pencil "beamlets" that lead to dose delivery in tissue using highly converged Monte Carlo. Coupling the EDKs to accumulate dose scaled by integral photon fluences computed using S_N methods in dose driving voxels (DDVs) allows for the full charged particle physics computed dose to be accumulated throughout the voxelized phantom, and is the basis of the EDK-SN method, which is fully parallelized. For material heterogeneities, a density scaling correction factor is required to yield good agreement. In a fully voxelized phantom, all doses were in agreement with those determined by independent Monte Carlo computations. We are continuing to expand upon the development of this robust approach for rapid and accurate determination of whole body and out of field organ doses due to high energy x-ray beams.

KEYWORDS: 3-D, Deterministic S_N, EDK-S_N, Whole Body Dose, Heterogeneities

1. INTRODUCTION

A novel methodology was recently developed by our research team called EDK-S_N, or "Electron Dose Kernel Discrete Ordinates" [13]. The purpose of this methodology is to rapidly and accurately estimate organ doses anywhere in the human body, and attribute whole body doses incurred from very high energy photon beams typical of those used in external beam therapy. The methodology employs CT-based voxelized anatomical patient phantoms, and doses are computed in a two step process. In the first step, we rapidly solve for the photon transport deterministically over the entire phase space of the phantom using 3-D discrete ordinates (S_N) radiation transport on parallel computer architectures. The photon transport is achieved using the PENTRAN-MP code system [4]. In the second step, the highly detailed angular data rendered globally over the phantom from the S_N solution is used to project the dose and map it to surrounding voxels; the dose is accumulated on a mesh by mesh basis, scaled by the magnitude of the photon fluence, using Electron Dose Kernels (EDKs). EDKs were precomputed for the EDK-S_N methodology using full phsyics charged particle Monte Carlo electron transport for a single mono-energetic pencil photon beam in either soft tissue, bone, or lung tissue, and adapted to any radiation direction on the unit sphere so as to enable coupling to photons traveling in any direction, as determined via S_N photon transport computations. This technique was successfully

demonstrated in detailed comparisons with independent Monte Carlo photon-electron transport calculations for single masses of soft tissue [13]. The focus of work here is to present testing and validation of the EDK-S_N method to accurately calculate the dose deposited to account for material interfaces and heterogeneities. Subsequent sections present background, test results, discussion, conclusions, and references.

2. BASIS OF THE EDK-S_N METHOD

For low energy photons, Charged Particle Equilibrium (CPE) usually exists within the patient treatment volume. With CPE on a voxelized human phantom with mesh voxels on the order of 1 cm^3, the photon absorbed dose is equal to the collisional kerma, and the dose can therefore be readily obtained using flux-to-dose conversions, since secondary electrons created as a result of the primary photon interactions deposit their energy locally, and no charged particle transport is necessary. However, this is not true for the dose buildup region near the surface of the patient, or at interfaces of dissimilar materials such as tissue/lung, where corrections for secondary electron transport may be significant [1,2,3,6].

In addition, as higher photon beam energies are considered, photons in a voxel of the phantom, which we label the "dose driving voxel," or DDV, cause secondary electrons be created that can undergo significant amounts of transport as they slow and deposit energy. Those secondary electrons transport through the phase space, primarily along the direction of the net photon current in the DDV, where we note that photon scattering is increasingly forward peaked with increasing photon energy. With continued charged particle transport, the secondary electrons transport deeper into the surrounding tissue, and ultimately are slowed to rest, depositing energy in phantom voxels distal from the DDV to create a net tissue dose. The fate of the secondary electrons from their point of creation in the DDV, undergoing charged particle transport, depositing dose in tissue at points distal from where they were created, is a very difficult challenge to model deterministically; this must be handled using a non-linear form of the Boltzmann equation, such as the Boltzmann-Fokker-Planck equation. While computationally and therefore very time intensive, charged particle transport has been very accurately solved using condensed history Monte Carlo transport methods. Alternatively, deterministic *neutral particle* transport, while challenging to achieve on a large 3-D geometry, is not nearly as difficult and can be rapidly solved using parallel computing architectures.

Deterministic discrete ordinates approximations of the neutral particle transport equation invoke a discretization of the energy, angle, and space variables. Discretization of energy is accomplished by spectrally averaging over energy groups ($g=1,G$), from high to low energies, resulting in the multigroup transport formulation. In steady state, the multigroup transport equation is

$$\hat{\Omega}\cdot\nabla\psi_g(\vec{r},\hat{\Omega})+\sigma_g(\vec{r})\psi_g(\vec{r},\hat{\Omega})=\sum_{g'=1}^{g}\int_{4\pi}d\Omega'\sigma_{s\,g'\to g}(\vec{r},\hat{\Omega}'\cdot\hat{\Omega})\psi_g(\vec{r},\hat{\Omega}')+q_{ind\,g}(\vec{r},\hat{\Omega}) \quad (1)$$

where the left side includes loss by leakage and collision, with scatter and independent sources on the right. In addition to multigroup energy discretization, the S_N method also provides for discretization of the angular domain over a number of discrete directions and spatial cells

(voxels). Since angular data is obtained from a detailed solution of the neutral particle Boltzmann solver, it is readily available and explicitly stored in scalable parallel data arrays in the PENTRAN S_N code; our two-step EDK-S_N "electron kernel" treatment described in Section 1 can be applied to effectively attribute dose from high energy photons. Mitigating issues in accomplishing this correctly must be defined based on meshing, proper quadrature sets, cross section libraries, and S_N differencing schemes; these issues have already been investigated in assessing what is typically required to yield accurate photon transport [7].

To properly treat the physics deterministically, yet still to achieve reasonably fast and accurate whole body computation times using high energy photons, energy dependent electron transport dose "kernels" are pre-computed using Monte-Carlo to extremely low variances within tissue media. These Electron Dose Kernels (EDKs) are derived using full physics charged particle Monte Carlo electron transport for a single, mono-energetic pencil photon beams in soft tissue, bone, and lung tissue. Then, EDKs are scaled to any radiation direction on the unit sphere so as to enable coupling via projection for photons along specific directions of travel (determined from the net photon current vector) rendered from solution of the Boltzmann transport equation. This permits complete accumulation of the dose due to charged particle transport along a photon net current vector direction, with energy depositing in voxels distal from the original photon location (*i',j',k'*), as depicted in Fig. 1.

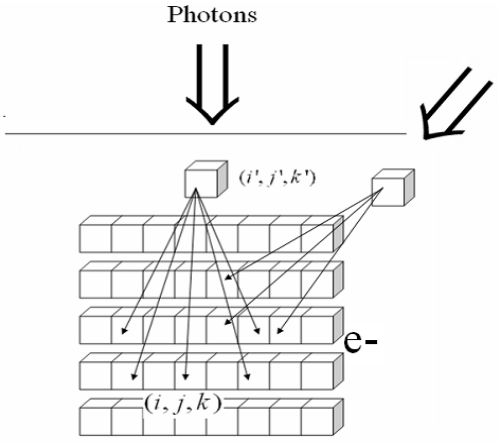

Figure 1. Schematic of photons in a 'dose driving voxel' (DDV) at location (*i',j',k'*) creating charged particles and energy deposition in voxels distal from the DDV

The EDK coupled with S_N (EDK-S_N) method essentially provides an "equivalent electron dose look-up" for each photon "beamlet" in a discrete ordinates computation. Specifically, the net photon current vector is readily determined from the S_N computation, and in Cartesian geometry is denoted by:

$$\vec{J}_n = J_{nx}\,\hat{i} + J_{ny}\,\hat{j} + J_{nz}\,\hat{k} \tag{2}$$

In addition, the electron dose kernel fraction in distal voxels (*i, j, k*), given as EDF_g, due to a primary photon at (*i',j',k'*), can be determined in terms of the initial photon energy for a particular energy group g. By partitioning the energy deposited in voxel (*i, j, k*), into multiple

energy bins equivalent to the S_N multigroup energy structure, we can construct the fractional electron dose kernel contribution per unit photon flux (based on Monte-Carlo) per source particle:

$$EDF_g(i,j,k) = EDK_g(i,j,k) \Big/ \phi_{MC_g}(i',j',k') \tag{3}$$

The transport-guided dose rate $\dot{D}(i,j,k)$ can then be obtained for each voxel location (i, j, k) by summing the product of the $EDF_g(i,j,k)$, the β, a particle normalization factor, and the S_N scalar flux $\phi(i,j,k)_{S_{Ng}}$, divided by the voxel mass M (i, j, k):

$$\dot{D}(i,j,k) = \sum_g \left(\sum_g EDF_g(i,j,k)_S\right)\left(\phi(i,j,k)_{S_N g}\right)\beta / M(i,j,k) \tag{4}$$

This procedure enables the detailed information to be obtained on the dose deposited in the model. The EDK-S_N methodology is indeed similar to the traditional convolution–superposition technique, which applies a database of "energy deposition kernels," calculated using Monte Carlo techniques to determine a dose [8,9]; however, the convolution–superposition technique is performed without regard to the incident photon angular components, and so can be in serious error as photon energies increase. Alternatively, the EDK-S_N procedure is based on a highly detailed, full physics Boltzmann photon transport solution with direction and flux information directly available for coupling with the EDKs along the propagated photon current direction.

The EDK-S_N methodology serves as a critical link in a system to accumulate the absorbed dose in each fine mesh. Accumulation of the dose in each voxel of tissue is performed using two protocols:

I. For low photon energies, where CPE conditions are absolutely met, the algorithm will apply a simple collisional kerma approximation based on pre-calculated 3-D fluxes/fluences determined directly from our 3-D S_N methods. A deterministically derived dose will be accurate up to the range of the electron path lengths in the material of interest, and comparable to ranges smaller than the spatial S_N mesh grid interval in anatomical models (representative of the anatomic data voxel size).

II. At high energies were CPE conditions is not valid, the EDK-S_N procedure will be applied, and the accumulated energy deposited in each voxel for each photon energy group will be based on the S_N computed photon flux and projected dose due to electrons streaming along the photon current vector, as described.

3. EVALUATION OF HETEROGENEOUS PHANTOMS

Because the EDK-S_N calculation is performed over the full spectrum of the radiation for a discrete number of energy groups, we can generate separate sets of electron absorbed dose kernels (EDKs) to account for different densities present in the phantom model. In this section, we address applying the EDK-S_N method to a heterogeneous phantom, including the application

to a new state of the art human phantom. Three 'slab based' phantoms were simulated, using the EDK-S_N method, as a prelude to more complex calculations for full human phantoms. These slab phantoms each used a flat-weighted 0 to 8 MV x-ray incident source. The phantoms were 45x45x45 cc in size, and are composed of 1-cm-thick soft tissue (S) discs, and materials representative of 1cm sections of bone (*B*), or lung tissue (*L*). The slab phantoms are depicted in Fig. 2.

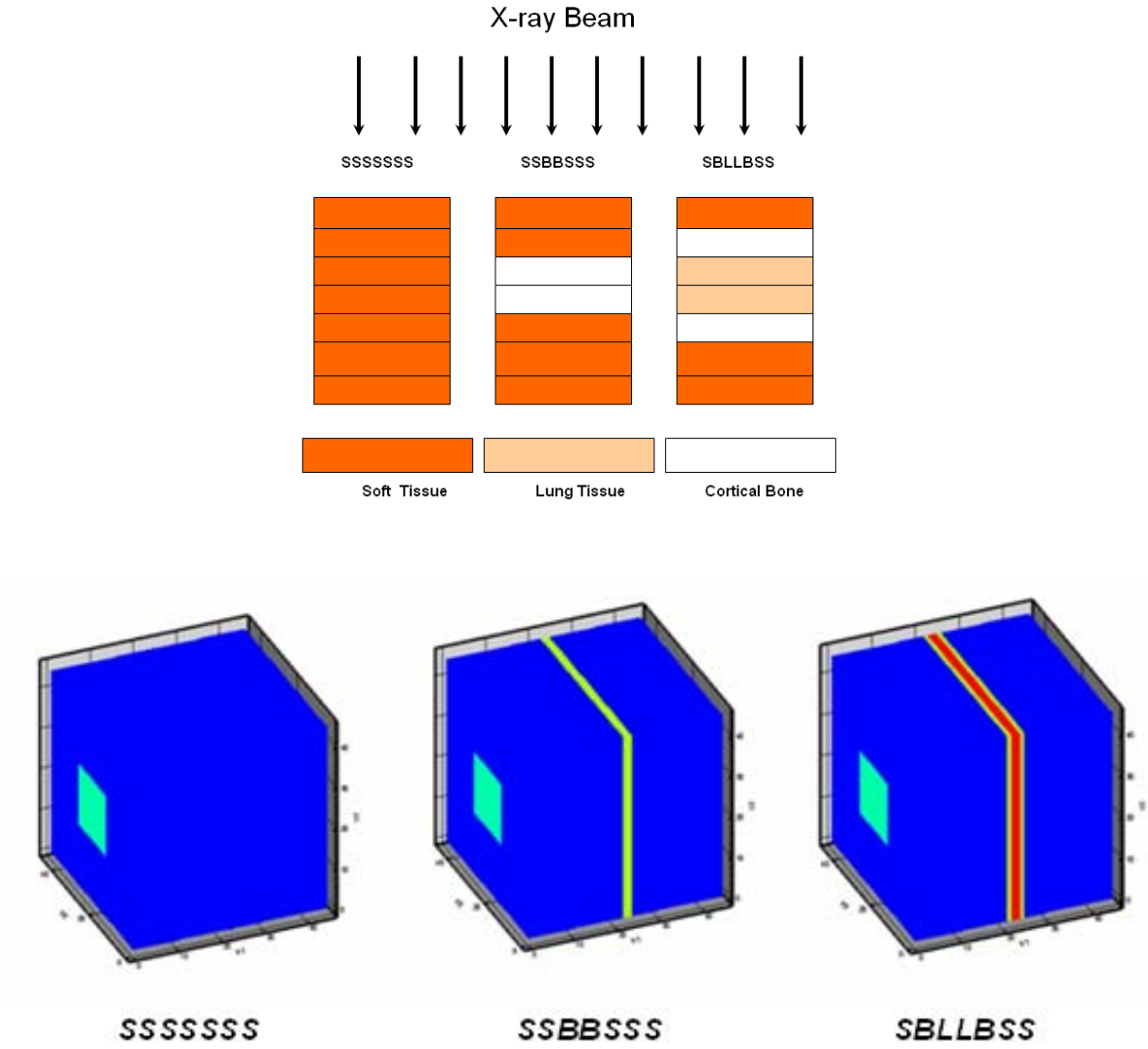

Figure 2. (Top) Schematic of three phantoms for heterogeneous absorbed dose studies. Phantom *SSSSSSS* is a homogeneous soft-tissue ('S') phantom; phantoms *SSBBSSS* and *SBLLBSS* include combinations of 1 cm sections of soft tissue ('S'), bone ('B'), and lung ('L') tissue-equivalent materials, respectively; (Bottom) 3-D model of the heterogeneous phantoms, and the beam source plane is shown on the left edge [14].

3.1 Monte Carlo Simulations

In order to assess the accuracy of the EDK-S_N methodology in heterogeneous phantoms, a series of Monte Carlo simulations were performed using the radiation transport code MCNP5 to provide a benchmark for comparison. An X-ray flat weighted spectrum 8 MV used as input to MCNP5 to guarantee that no specific preference was given to any particular energy group. Volumetric cell estimates of tissue absorbed dose were calculated in MCNP5 by tallying the energy deposited by the photons and secondary electrons within 1 cm^3 voxels, equivalent to the size of the EDK-S_N voxels and the voxel sizes to be used in the S_N calculations.

After running the three phantoms for 500 minutes total on a 16 processor parallel cluster, the Monte Carlo uncertainty (2σ) was reduced to 10% on average along the axis of the radiation beam (Fig. 3). The Monte Carlo based computed difference in the deposited dose between the two tissues is within 2% for all phantom geometries, making it challenging to observe differences between the different tissues in the phantoms, especially for therapeutic photon beams; this is clearly evident in Fig. 4. The estimated time required to reduce Monte Carlo uncertainty to (2σ) 2% on-axis was 12500 minutes on 16 processors; hence, the computer time required to reduce the Monte Carlo uncertainty off-axis to 2% or less will be much greater. Therefore, this highlights the fact that tissue heterogeneities can be difficult to discern in these types of problems using the full physics Monte Carlo method, and computation times can be quite large to yield highly accurate charged particle transport solutions.

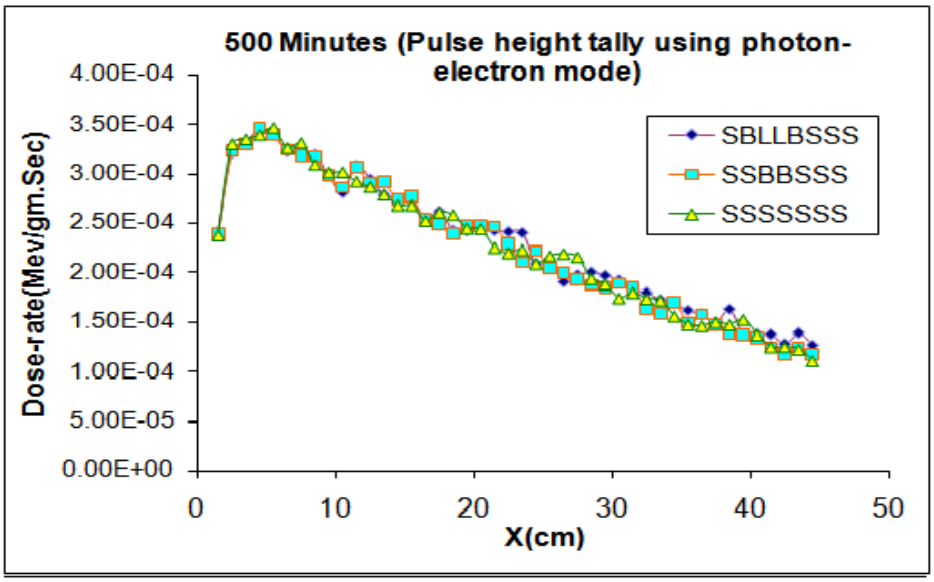

Figure 3. Monte Carlo derived total absorbed dose rate distributions along the x-axis computed using *F8 MCNP5 tally for three different phantoms. MCNP uncertainty (2σ) average (10.0%), 500 Minute run, 16 processors.

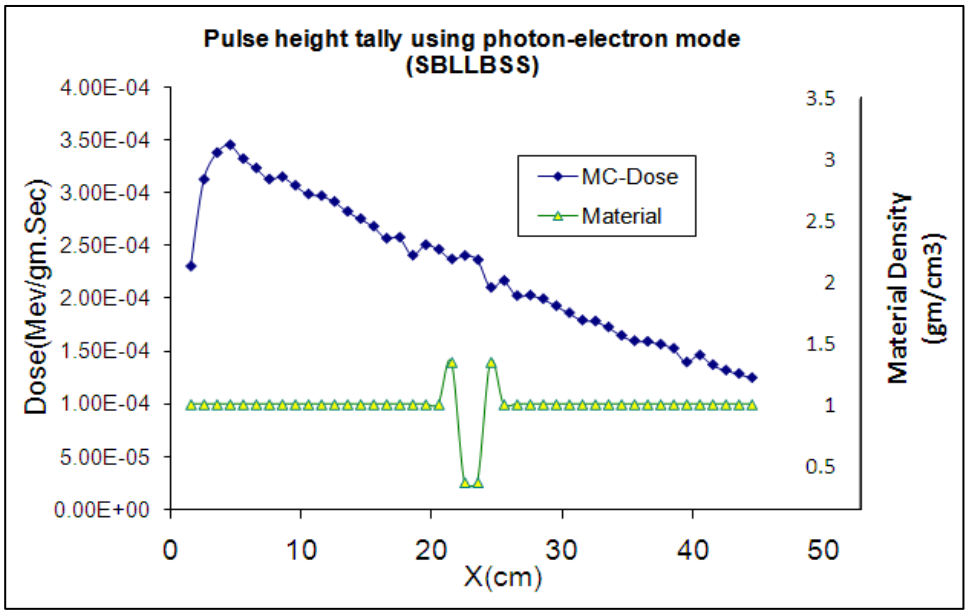

Figure 4. Monte Carlo derived total absorbed dose rate distributions along the x-axis computed using *F8 MCNP5 tally for the 'SBLLBSS' slab phantom. MCNP uncertainty (2σ) average (7.0%), 1000 Minute run, 16 processors.

One of the most important issues limiting the use of the Monte Carlo techniques for clinical absorbed dose calculations is achieving a statistically reliable result in a reasonable time. This problem is even greater when a photon-electron mode is required, when CPE is not applicable, causing computer running times needed to reduce the statistical error to increase rapidly. Improved variance reduction techniques may reduce the computation times. However, such techniques are to be used with caution, as improper application of statistical variance reduction may cause wrong answers. Moreover, variance reduction techniques may not reduce the time required to reduce the variance to acceptable levels, especially when accurate absorbed dose estimations are needed globally over the entire problem (phantom).

3.2 PENTRAN S_N Model

We simulated three phantoms equivalent to those in Fig. 2 simulated with Monte Carlo using S_N transport solved using the PENTRAN code. The heterogeneous models consisted of three key components; an X-ray source ($15\times1\times15$ cm^3) with a flat weighted 8 MV source, divided into 16 energy groups, a soft tissue phantom ($45\times45\times45$ cm^3), and equivalent layers of bone and lung tissue identical to those in the Monte Carlo simulations. Models were divided into 3 z-levels; each z-level was divided equally into 9 coarse meshes containing ($15\times15\times15$) fine mesh cells for each coarse mesh; a total of 91,125 fine mesh cells were used in the S_N problems. Although comparatively lower quadrature orders (S_{32}) are sufficient to produce accurate S_N results for similar calculations, to minimize the potential for ray-effects in the S_N calculations, these simulations utilized an S_{62} angular Legendre-Chebychev quadrature with P_3 scattering anisotropy and a CEPXS generated library.

3.3 Applications of the EDK-S_N Procedure with Heterogeneities

EDK-S_N dose calculations were performed for the slab phantoms using material specific absorbed dose kernels, making use of pre-computed electron absorbed dose kernels for different densities in the phantom model. The dose rate in the all-tissue 'SSSSSSS' phantom, comparing EDK-S_N and Monte Carlo results, is shown in Figure 5; agreement was excellent, and the average relative difference in dose was within a (2σ) statistical Monte Carlo uncertainty.

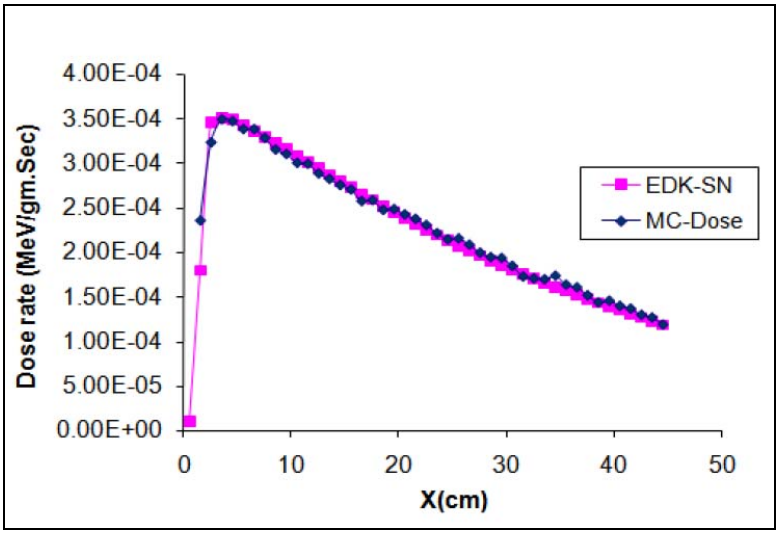

Figure 5. Comparison of EDK-SN dose with on-axis Monte Carlo dose (MCNP *F8 tally) for the 'SSSSSSS' slab phantom. MCNP uncertainty (2σ) average (6.0%), Average absolute relative difference (3.7%).

Comparing the dose rate in the mixed material 'SBLLBSS' phantom revealed that the EDK-S_N and Monte Carlo dose differed in the vicinity of the material change (Fig. 6, top). By investigating this difference more thoroughly, evaluating the dose and electron ranges for various photon energies in tissue, lung, and bone, our team developed a density scaling procedure for the EDK-S_N method. This density scaling procedure is as follows: when the DDV differs from the surrounding mesh, a density ratio is applied to the dose accumulated in distal voxels to account for material heterogeneities. This treatment successfully yields an accurate dose, as noted in Fig. 6 (bottom).

The EDK-S_N methodology, with density corrections for material heterogeneities, was then applied to a fully voxelized phantom and compared with MCNP5 results for a high energy volumetric (20×1×17 cm^3) flat weighted source [0,8 MeV]. The phantom, initially 2×2×2 mm^3 (302×139×836 voxels), was down sampled to 1×1×1 cm^3 (60×27×167 voxels), for total of 270,540 voxels; this is shown in Figure 7. Dose Results are indicated in Table 1, which reveal that all doses were comparable within a Monte Carlo (2σ) uncertainty, except for the spleen prostate. Monte Carlo prostate doses were not converged, since this organ was far out of field; subsequent simulations requiring an additional ~40 h on 16 processors demonstrated the Monte-Carlo result was converging to the EDK-S_N result. This demonstrates the power of the EDK-S_N method, since it required a total of 2 h (1.5 h parallel S_N / 0.5 h parallel EDK) to yield whole body doses. More investigations of the accuracy of the EDK-S_N method are continuing.

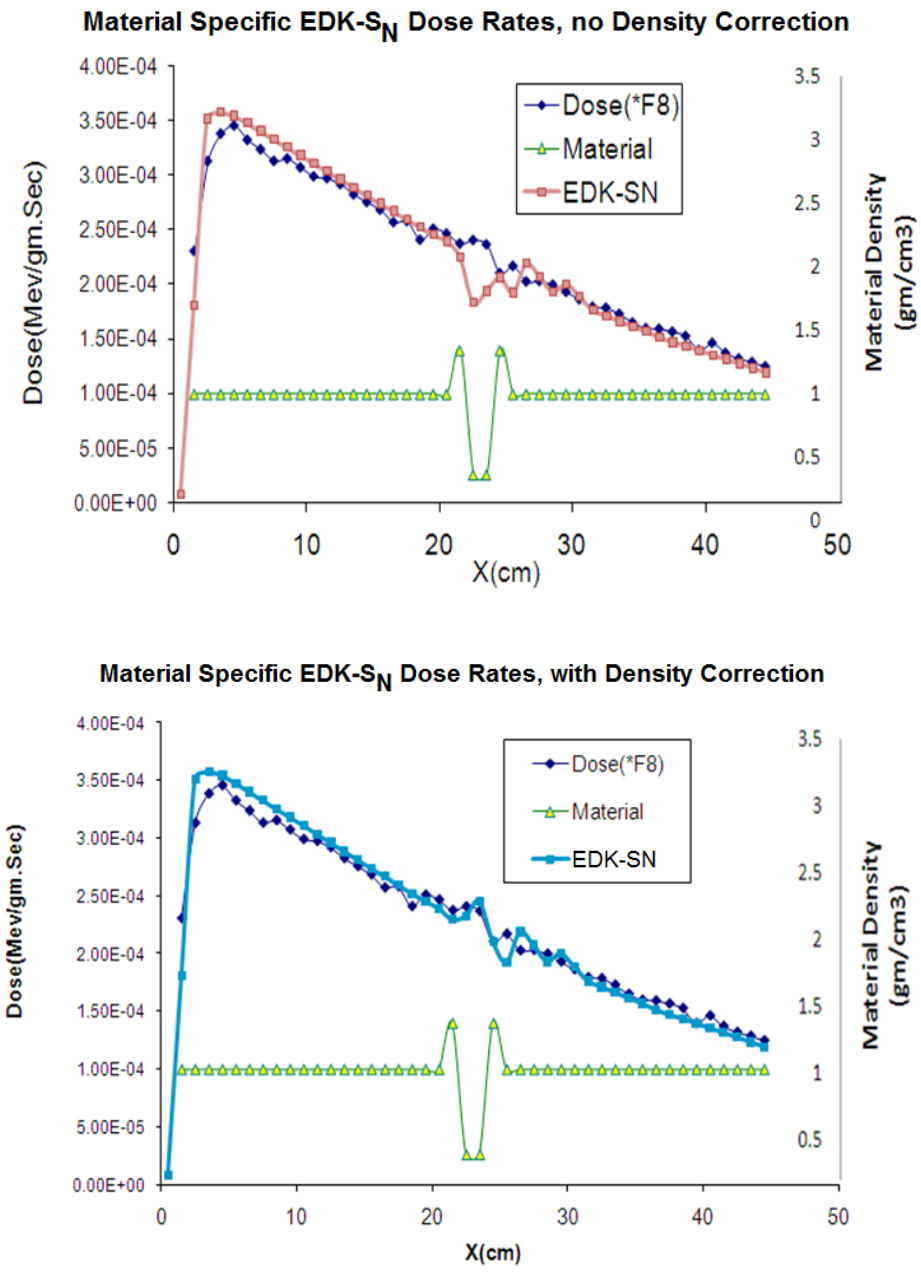

Figure 6. (*Top*) EDK-S_N Heterogeneous 'SBLLBSS' phantom total absorbed dose rate (without correction factor) along the x-axis compared to MCNP *F8 tally dose rate. MCNP uncertainty (2σ) average (8%) on-axis. Average absolute relative difference (4.1%); (*Bottom*) EDK-S_N Heterogeneous 'SBLLBSS' phantom total absorbed dose rate *with density correction applied, a*verage absolute relative difference (<4.0%).

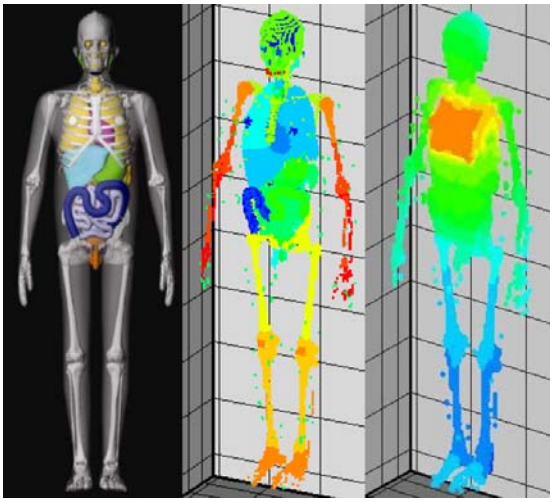

Figure 7. Simulation methodology for EDK-S_N computations using PENTRAN-MP code system. (Left) UF Anthropomorphic phantom; (middle) corresponding PENTRAN input, (right): EDK-S_N absorbed dose distribution after application of high energy x-ray source

Table 1. Comparison of selected organ absorbed dose rate (MeV/g.s) calculated using MCNP5 pulse height tally with (photon, electron mode) and EDK-S_N for the UF hybrid 15-year-old male phantoms for 8 MV X-ray Source

Organ	MC(*F8) (MeV/g.Sec)	(2-sigma) MC Uncertainty	Sn-EDK (MeV/g.Sec)	(MC-EDK)/EDK
Right+ Left Lung	1.35E-01	6.80%	1.41E-01	4.56%
Pancreas	9.47E-05	4.14%	9.85E-05	4.02%
SI W	3.56E-05	4.00%	3.75E-05	5.43%
Spleen	1.11E-04	3.00%	1.18E-04	6.58%
Stomach W	1.86E-04	4.60%	1.94E-04	4.09%
Thyroid	1.41E-05	6.82%	1.38E-05	2.08%
Prostate	2.21E-08	44.00%	2.29E-08	3.62%

4. CONCLUSIONS

In this paper, we presented the EDK-S_N method to rapidly compute doses and account for material heterogeneities in phantoms irradiated by high energy external photon beams. Use of the pre-computed EDKs allows for the full charged particle physics dose to be accumulated throughout the voxelized phantom based on a rapidly computed S_N solution. To properly attribute dose due to material heterogeneities in applying the EDK-S_N method, a density scaling correction factor was required to yield good agreement with Monte Carlo results. In a fully voxelized phantom problem, all doses were in agreement with those determined by independent Monte Carlo computations when the Monte Carlo results were well converged. We are continuing to expand upon the development of this robust approach for rapid and accurate determination of whole body doses using high energy x-ray beams.

REFRENCES

[1]T. R. Mackie, P. Reckwerdt, and N. Papanikolaou, "3-D Radiation Treatment Planning and Conformal Therapy," *Medical Physics Publishing Corporation* Madison WI, p. 34, (1995).

[2]B. A. Fraass, J. Smathers, and J. Deye, "Summary and recommendations of a National Cancer Institute workshop on issues limiting the clinical use of Monte Carlo dose calculation algorithms for megavoltage external beam radiation therapy," Med Phys **30,** 3206-3216 (2003).

[3]C. M. Ma, E. Mok, A. Kapur, T. Pawlicki, D. Findley, S. Brain, K. Forster, and A. L. Boyer, "Clinical implementation of a Monte Carlo treatment planning system," Med Phys **26,** 2133-2143 (1999).

[4]A. Al-Basheer, G. Sjoden, M. Ghita, "Critical Discretization Issues in 3-D S_N Simulations Relevant to Dosimetry and Medical Physics", (accepted) *Nuclear Technology Journal,* 32 pages (manuscript), (2008)..

[5]G. M. Daskalov, R. S. Baker, R. C. Little, D. W. O. Rogers, and J. F. Williamson, "Two-Dimensional Discrete Ordinates Photon Transport Calculations for Brachytherapy Dosimetry Applications," Nucl. Sci. Eng. **134,** 121-134 (2000).

[6]F. H. Attix, "Energy imparted, energy transferred and net energy transferred," Phys Med Biol **28,** 1385-1390, (1983).

[7]A. Al-Basheer, M. Ghita, and G. Sjoden, "Investigation of deterministic simulation parameters for a 3-D radiotherapy Co-60 device model," in *ANS Winter Meeting and Nuclear Technology Expo*, Albuquerque, NM, pp. 511-513 (2006).

[8]T. R. Mackie, A. F. Bielajew, D. W. Rogers, and J. J. Battista, "Generation of photon energy deposition kernels using the EGS Monte Carlo code," Phys Med Biol **33,** 1-20 (1988).

[9]A. Ahnesjo, P. Andreo, and A. Brahme, "Calculation and application of point spread functions for treatment planning with high energy photon beams," Acta Oncol **26,** 49-56 (1987).

[10]LANL X-5 Monte Carlo Team, *MCNP5- A General Monte Carlo N-Particle transport code, Version 5*, Los Alamos, NM (2006).

[11]B. Wang, G. Xu, J. T. Goorley, and A. Bozkurt, "ISSUES RELATED TO THE USE OF MCNP CODE FOR AN EXTREMELY LARGE VOXEL MODEL VIP-MAN," in *The Monte Carlo Method: Versatility Unbounded In A Dynamic Computing World*, American Nuclear Society, Chattanooga, Tennessee, pp. 32 (2005).

[12]G. Sjoden, and A. Haghighat, "PENTRAN - A 3-D Cartesian Parallel SN Code with Angular, Energy, and Spatial Decomposition," in *Int'l. Conf. on Math. Meth & Supercomp. for Nuclear App.*, edited by Saratoga Springs, New York, (1997).

[13]A. Al-Basheer**, G. Sjoden, and M. Ghita, “Electron Dose Kernels to Account for Secondary Particle Transport in Deterministic Simulations”, *accepted*, *Nuclear Technology Journal*, January, 2008, 19 pages.

[14]A. Al-Basheer, "3D DETERMINISTIC RADIATION TRANSPORT FOR DOSE COMPUTATIONS IN CLINICAL PROCEDURES," Ph.D. Thesis in Nuclear and Radiological Engineering, University of Florida, August, 2008.